Available online at www.sciencedirect.com
SCIENCE DIRECT®
PERGAMON
Geothermics 33 (2004) 655–673
GEOTHERMICS
www.elsevier.com/locate/geothermics

Chemical and isotopic composition of geothermal discharges from the Puyehue-Cordón Caulle area (40.5°S), Southern Chile

Fabián Sepúlveda [a,*], Klaus Dorsch [b], Alfredo Lahsen [a], Steffen Bender [b], Carlos Palacios [a]

[a] *Department of Geology, University of Chile, P.O. Box 13518, 21 Santiago, Chile*
[b] *Department of Geo- and Environmental Science, Ludwig-Maximilians University of Munich, Luisenstr. 3780333 Munich, Germany*

Received 5 March 2003; accepted 29 October 2003

Available online 10 May 2004

Abstract

The Puyehue-Cordón Caulle area (40.5°S) hosts one of the largest active geothermal systems of Southern Chile, comprising two main thermal foci, Cordón Caulle and Puyehue. Cordón Caulle is a NW-trending volcanic depression dominated by fumaroles at the top (~1500 m) and boiling springs at the northwest end (~1000 m). In the latter, the alkaline-bicarbonate composition of the springs with low Mg (<0.06 mg/l) relative to the local meteoric waters (~5 mg/l), low chloride (<60 mg/l), high silica (up to 400 mg/l) and $\delta^{18}O$–δD values close to the Global Meteoric Water Line (GMWL), in combination with the large outflow (100 l/s), suggest the existence of a secondary steam-heated aquifer overlying a main vapor-dominated system at Cordón Caulle. Subsurface temperatures of the secondary aquifer are estimated to be about 170–180 °C (corrected silica geothermometers). The Puyehue thermal area, on the other hand, includes Mg-rich hot springs discharging along stream valleys, with maximum temperatures of 65 °C and a $\delta^{18}O$–δD signature resembling the local meteoric composition, which suggests that the surface manifestations contain a reservoir component that is strongly diluted by meteoric waters. Topographic/hydrologic and chemical characteristics suggest that Cordón Caulle and Puyehue represent two separate upflows.

Keywords: Chloride; Acid-sulfate; Bicarbonate; Heat loss; Reservoir; Temperature; Silica sinter; Geochemistry; Puyehue; Cordón Caulle; Chile

* Corresponding author. Tel.: +56-2-6784116; fax: +56-2-6963050.
E-mail address: fsepulve@cec.uchile.cl (F. Sepúlveda).

0375-6505/$30.00 © 2004 CNR. Published by Elsevier Ltd. All rights reserved.
doi:10.1016/j.geothermics.2003.10.005

1. Geological background

In 1999 the Department of Geology of the University of Chile initiated a geothermal research program aimed at characterizing and assessing the geothermal resources of Central-Southern Chile. Several areas were identified on the basis of existing literature (Lahsen, 1988; Hauser, 1997; Pérez, 1999) and geological reconnaissance surveys. Of these, the Puyehue-Cordón Caulle area (40.5°S) was found to be one of the most promising due to the wide diversity of its surface manifestations. The chemical data from hot springs and isotopic data from both hot springs and fumaroles are reported in this study. A conceptual model of the deep geothermal system has been developed on the basis of these data.

The thermal activity of the Puyehue-Cordón Caulle area is grouped within the Cordón Caulle area, to the north, and the Puyehue area, 15 km further south (Fig. 1). The relationship between thermal activity and recent volcanism is particularly clear in the Cordón Caulle area, which lies over a flat-topped volcanic depression (or plateau) bordered by NW-trending faults. Both the monogenetic volcanic centers and the thermal manifestations show a remarkable spatial relationship with this NW-oriented structural corridor (Fig. 1). In particular, post-glacial and historic (1921–1922 and 1960) dacitic-to-rhyolitic fissure lavas and lavadomes have been erupted from the southwestern border of the plateau, the so-called Cordón Caulle Fissure (Moreno, 1977; Fig. 2). With the exception of the historic lavas, most of the Cordón Caulle area is blanketed by pumice layers. The Cordón Caulle area is bounded to the southeast by the Puyehue strato-volcano (2236 m), the bulk of which is made up of numerous intra-glacial basaltic lavas that have accumulated over a pre-existing ∼5 km wide caldera. The Puyehue volcano initiated a post-glacial explosive stage, leading to the current morphology of the volcano with a ∼2.5 km wide caldera, followed by more effusive andesite and dacite flank eruptions. Northwest of Cordón Caulle is the ∼10 km wide Cordillera Nevada volcanic group (Fig. 1), representing the remnant of a collapsed strato-volcano with pre-caldera sequences dating back to about 1 Ma (Campos et al., 1998; Lara et al., 2001). The transition from basaltic to felsic volcanism in the post-glacial lapse, both in the Puyehue volcano and Cordón Caulle areas, is believed to be associated with the onset of geothermal activity.

The Casablanca-Antillanca volcanic complex consists of a Late Pleistocene-to-Holocene basaltic strato-volcano (1990 m) and multiple post-glacial monogenetic, flank- and fissure-related scoria cones (e.g. López-Escobar et al., 1995; Lara et al., 1999; Fig. 1). Thick sequences of basaltic flows interbedded with laharic deposits are particularly well exposed on the southern shore of Lake Puyehue (Fig. 1). The Puyehue thermal area is spatially related to the Casablanca-Antillanca group but the genetic connection is uncertain.

The basement of Cordón Caulle and Puyehue comprises mainly Miocene intrusions, which crop out to the west, in the Lake Puyehue area, and to the east, along the NNE-trending Liquiñe-Ofqui Fault Zone (Cembrano et al., 1996, 2000; Fig. 1). An Ar–Ar age of 5.44 ± 0.02 Ma has been obtained in an intrusion cropping out west of the Lake Huishe area (Fig. 1). Both plutonic fragments contained in strombolian deposits, south of the Puyehue Volcano, and plutonic inclusion-bearing basaltic bombs of the northern Carrán-Los Venados group (Fig. 1), provide some insight into these deep intrusions underneath the Puyehue and Cordón Caulle areas. Plutonic clasts are often hydrothermally altered with secondary epidote and chlorite, which suggests water-rock interaction at high-temperature (>200 °C).

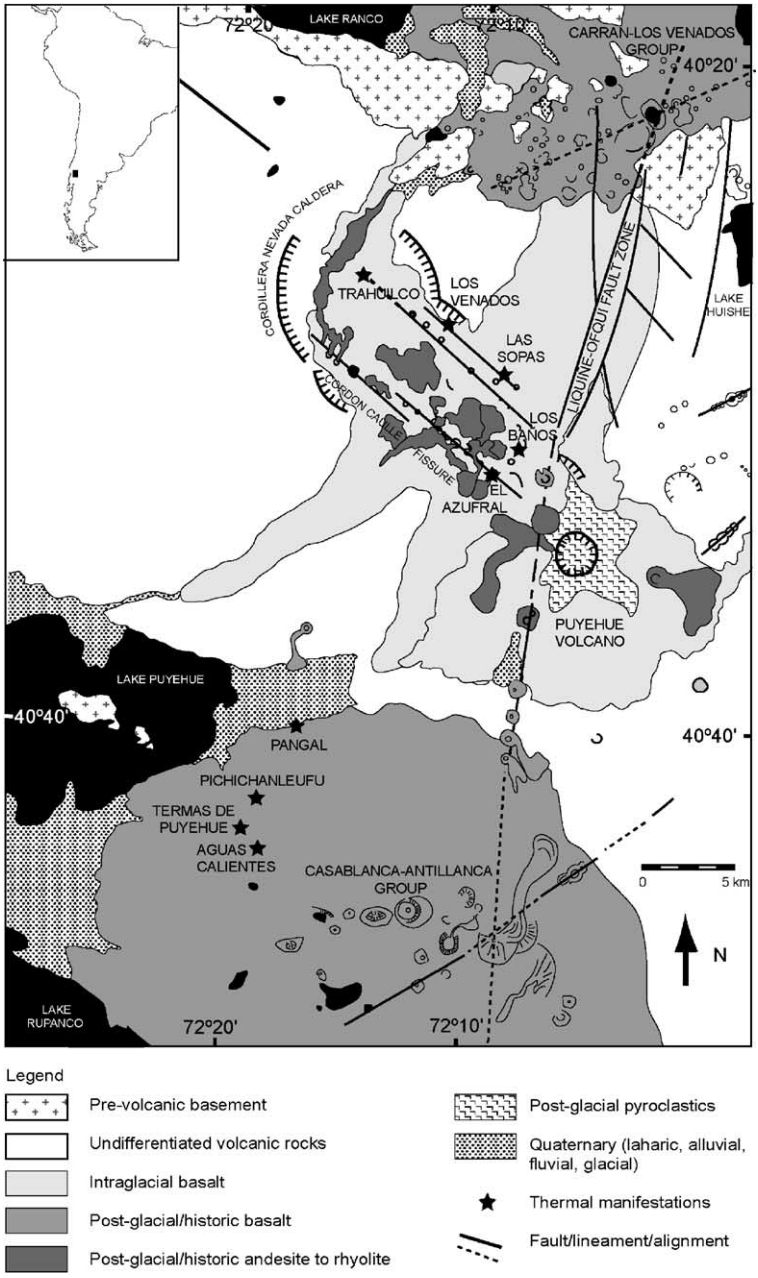

Fig. 1. Geological map of the Puyehue-Cordón Caulle region (after Moreno, 1977).

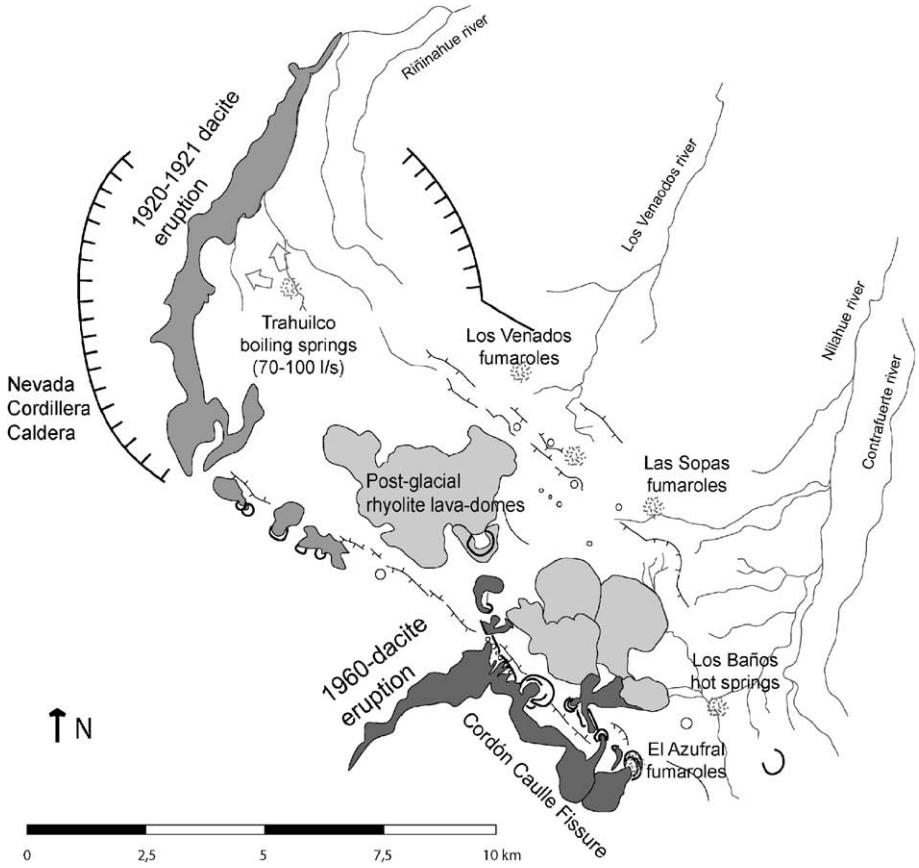

Fig. 2. Map showing the distribution of the main thermal zones of the Cordón Caulle area, and the location of post-glacial and historic eruptions.

2. Surface manifestations

Altogether, the surface manifestations of the Puyehue and Cordón Caulle areas occupy an area of 60 km^2. The Cordón Caulle area includes the following thermal zones, from northwest to southeast: Trahuilco (1050 m), Los Venados (1514 m), Las Sopas (1530 m), Los Baños (1430 m) and El Azufral (1650 m; Fig. 2). With the exception of Los Baños, these thermal zones align in a NW trend, in association with the NW-trending borders of the graben of Cordón Caulle. Other minor thermal zones (mainly diffuse steam exhalations) can also be found at Cordón Caulle. Acid-sulfate alterations associated with diffuse steam emissions also occur over the northwestern flank of the Puyehue volcano, close to the summit. To a large extent, hydrothermal alteration is restricted to active geothermal vents, suggesting that Cordón Caulle is underlain by a relatively young geothermal system (<10,000 years).

Las Sopas and Los Venados consist of near-boiling fumaroles whose acid steam produces intense acid-sulfate alterations, consisting of elemental sulfur, kaolinite, smectite, alunite and minor pyrite. Acidic pools (pH 2–3) and mud pools (the term pool referring to thermal water with no apparent overflow) are also present at Las Sopas, their typical gray color indicating a large amount of suspended material. At Los Venados, a clear warm spring with a small overflow (<0.1 l/s?; sample LVs; Table 1) and conspicuous silica incrustations emerge from pumice layers, about 50 m away from the main fumaroles. El Azufral consists of fumaroles, diffuse gas discharges and solfataras, situated inside and over the northern flank of the cinder cone of El Azufral, which formed during the latest eruptive cycle of the Cordón Caulle Fissure, in 1960 (Moreno, 1977; Lara et al., 2000; Fig. 2).

Trahuilco is located inside the Cordillera Nevada Caldera. Radial faults are inferred from the presence of numerous dikes cutting the inner walls of the caldera. Intensively foliated lavas (up to ~100 fractures/m) cropping out around the fluid discharge areas, together with the structures referred to above, seem to provide permeable channels for the discharge of the thermal fluids. Alkaline waters (pH ~ 9), clear and blue in color (light scattering effect by silica in solution), are discharged from multiple boiling springs and geysers, with a total outflow that is estimated between several tens of liters up to ~100 l/s. The term geyser is used here to describe a particular variety of boiling spring showing frequent eruptive pulses, with a water column as high as 5 m. The heat discharged from the geysers and boiling springs of Trahuilco can be estimated as $Q = VC\Delta T$, where V is the average volumetric flow rate (l/s), $C = 4.19 \times 10^3$ (J/1 °C) is the thermal capacity of water, and ΔT is the difference between the discharge and ambient temperature (92 and 12 °C, respectively):

$$Q = 100\,(\mathrm{l/s}) \times 4.19 \times 10^3\,(\mathrm{J/1^\circ C}) \times (92 - 12)\,(^\circ\mathrm{C}) \sim 38\,\mathrm{MW_t}$$

This estimation is minimal for the Cordón Caulle area because it does not account for the evaporative heat loss from fumaroles (e.g. Las Sopas, Los Venados and El Azufral), and the heat discharged from other hot spring/pool areas (e.g. Los Baños).

Of particular interest is the occurrence of silica sinters and geyserites around the fluid discharge zones of Trahuilco. The existence of extinct, circular steep-sided craters made up of silica sinter, close to the active vents, indicates migration of activity through time. The XRD pattern of the sinters (see Appendix A) shows that Opal A, a variety of amorphous silica diagnostic of young deposits (<10,000 years; Herdianita et al., 2000a,b; Rodgers et al., 2002), is the dominant compound in the sinters.

Los Baños (samples LB1s and LB2s; Table 1) consists of clear bubbling (CO_2 output) hot springs and seepages discharging along one of the tributaries of the Nilahue River (Fig. 2), with surface temperatures in the range 45–70 °C, and a few diffuse steam emissions nearby. Algae growth occurs along the edges of the spring vents. Due to concealed discharges along the riverbed nearby, the outflow cannot be calculated accurately but is estimated to be lower than 10 l/s.

With the exception of Pangal, a 64 m deep private well (flow rate about 2 l/s), the surface manifestations of the Puyehue thermal area are only represented by hot springs discharging either along stream valleys, as in the case of Aguas Calientes and Pichichanleufu, or along fractured laharic deposits of the Casablanca-Antillanca group, as in the case of Termas de Puyehue (Fig. 1). Surface temperatures decrease with decreasing elevation moving

Table 1
Chemical and isotopic composition of geothermal discharges from the Puyehue-Cordón Caulle areas

Sample	Code	Type	pH	T (°C)	Elevation (m)	Na	K	Ca	Mg	Cl	SO_4	Carbonate alkalinity	SiO_2	B	Li	$\delta^{18}O$	δD	$T_{chalc.\ (1)}$	$T_{chalc.\ (2)}$	$T_{quartz\ (1)}$	$T_{quartz\ (2)}$	$T_{Na/K}$	$T_{K^2/Mg}$
Cordon Caulle																							
Los Baños 1	LB1s	Hot spring	6.5	70	1430	105	13.9	4.0	3.6	10	3	342	333	14.4	0.06								
Los Baños 2	LB2s	Hot spring	6.7	47	1430	122	13.3	8.2	4.9	56	13	342	146	8.7	0.10	−9.59	−68.9						
Las Sopas	LSp	Hot pool	3.3	94	1560	19.2	8.2	4.9	13.3	2	317	0	450	14.7	0.01	−3.39	−47.8						
Las Sopas	LSf	Condensate		94	1560											−8.82	−77.9						
Los Venados	LVs	Hot spring	8.8	30	1514	47	8	0.3	0.4	2	51	54	358	18.0	0.01	−9.39	−67.6						
Los Venados	LVf	Condensate			1514											−8.67	−81.1						
El Azufral	AZf	Condensate			1650											−8.35	−77.4						
Trahuilco 1	TR1bs	Boiling spring	7.8	91	1050	88	3.3	0.1	0.06	26	62	195	210	10.4	0.16	−9.13	−66.6	**163**		**184**		**165**	103
Trahuilco 2	TR2bs	Boiling spring	8.1	92	1050	101	3.1	0.1	0.01	11	27	208	259	12.0	0.19	−9.12	−69.6	**179**	**170**	**199**	**190**	**153**	127
Trahuilco 2	TR2bs	Boiling spring			1050											−9.18	−66.4						
Trahuilco 3	TR3g	Geyser	9.2	93	1050	140	4.4	0.1	0.01	12	32	210	409	15.4	0.32	−8.28	−65.0	**205**	**140**	**241**	**164**	**154**	139
Puyehue																							
Pichichanleufu	PIs	Hot spring	6.9	27	292	76	1.87	4.0	1.5	41	33	73	121	2.4	0.13	−8.19	−54.2	123		149		141	50
Pangal	PAw	Well	7.8	38	210	130	2.62	23.3	1.6	74	56	110	119	2.0	0.08	−7.94	−52.6	122		149		130	57
Puyehue	PUs	Hot spring	8.1	56	390	150	4.3	2.0	0.7	128	70	73	104	7.6	0.32	−8.73	−59.4	113		144		**149**	79
Puyehue	PUs	Hot spring			390											−8.62	−58.6						
Aguas Calientes 1	AC1s	Hot spring	6.9	64	510	159	7.5	10.0	1.4	135	88	64	131	2.0	0.46	−8.78	−59.2	128		152		**179**	83
Aguas Calientes 1	AC1s	Hot spring			510											−8.88	−58.2						
Aguas Calientes 1	AC1s	Hot spring			510											−8.83	−56.2						
Aguas Calientes 2	AC2s	Hot spring	7.2	48	490	148	7.1	8.8	1.0	110	91	79	89	6.6	0.40	−8.78	−58.4	104		139		**180**	85
Aguas Calientes 2	AC2s	Hot spring			490											−8.40	−55.0						
Melted snow	Snow	Melting water			1560											−8.73	−59.8						

Major element concentrations in mg/l; isotopic data in per million, relative to V-SMOW standard. pH correction with (1) H_4SiO_4 calculated at 25 °C, (2) H_4SiO_4 calculated at 92 °C.

northward from Aguas Calientes (62 °C; 510 m) through Termas de Puyehue (58 °C; 390 m) to Pangal-Pichichanleufu (27–30 °C; 210–290 m; Table 1).

3. Methods

Water samples were collected in polyethylene bottles of 500, 250 and 125 ml. Samples for cation and SiO_2 determinations were acidified with HNO_3. Before acidification, the samples were filtered with a 0.45 μm pore size membrane. Carbonate alkalinity ($HCO_3^- + CO_3^{2-}$) was analyzed on-site to prevent CO_2 loss effects, by acidic titration using H_2SO_4 and methyl-orange. On-site SiO_2 concentration was measured in the locality of Trahuilco ($pH > 8$), using a portable spectrophotometer, with the heteropoly blue method (reduction of silicomolybic acid by amino acid at 815 nm for high range and silicomolybdic acid at 420 nm for low range). Carbonate alkalinity was corrected for $H_3SiO_4^-$ titration in the alkaline waters. Fumarole condensates for stable isotopes were collected in 30–125 ml polyethylene and glass bottles connected to a spiral-shaped stainless steel condensing coil. Data set comparison suggests negligible isotope diffusion in polyethylene bottles. The analyses of water samples were carried out in the Hydrogeology Group of Ludwig-Maximilians University in Munich, Germany, by means of ion chromatography for anions; atomic absorption spectrometry for cations; and atomic emission spectrometry for Si. Stable isotope analyses in water samples were done in the laboratory of the UFZ Center for Environmental Research Leipzig-Halle, Germany, with an IR MS Delta S mass spectrometer using the EQ measuring method (CO_2 equilibration of the samples) against the V-SMOW standard. Fumarole condensates for isotope determination were analyzed in the laboratory of Thermochem, USA. The XRD diffractograms of silica sinter were obtained in the Geology Department of the University of Auckland, New Zealand.

4. Chemical and isotopic composition

The chemical and isotopic compositions of the geothermal discharges from the Cordón Caulle and Puyehue thermal areas are listed in Table 1. In general, all the samples have relatively low TDS (<600 mg/l) and particularly low chloride, specially at Cordón Caulle where Cl is lower than 60 mg/l. Regarding major anions Cl, SO_4 and HCO_3 (Fig. 3), Cordón Caulle is dominated by waters of the bicarbonate (e.g. Trahuilco and Los Baños) and sulfate type (e.g. Las Sopas). Mixed sulfate-bicarbonate waters are also present at Los Venados. In the Puyehue area, the samples are mixed Cl-HCO_3 SO_4 waters (Fig. 3).

The relative proportion of Cl and B, both regarded as conservative elements, is useful to trace the source of the thermal fluids. Because of its relative immunity to secondary processes, Li was chosen by Giggenbach and Goguel (1989) as a reference constituent to highlight the variations in the B/Cl ratios (Fig. 4). B/Cl ratios are higher in Cordón Caulle relative to Puyehue (Fig. 4), and absolute B concentrations in Cordón Caulle (9–18 mg/l) are a lot higher than the background levels detected in rivers and cold springs nearby ($B < 1.3$ mg/l; e.g. Nilahue river; Fig. 2). Plots of δD values against Cl (Fig. 5) are also

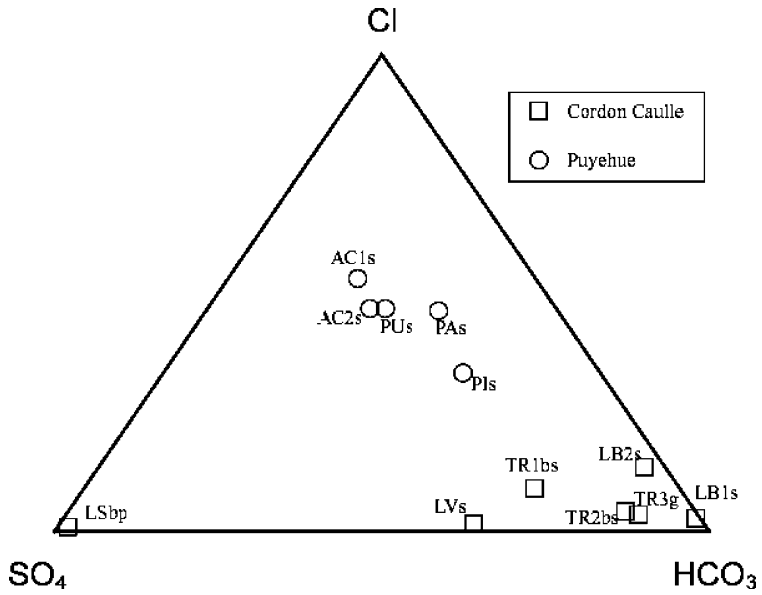

Fig. 3. Cl–SO_4–HCO_3 ternary diagram showing the main water types prevailing at Puyehue and Cordón Caulle. Note the overall absence of chloride waters.

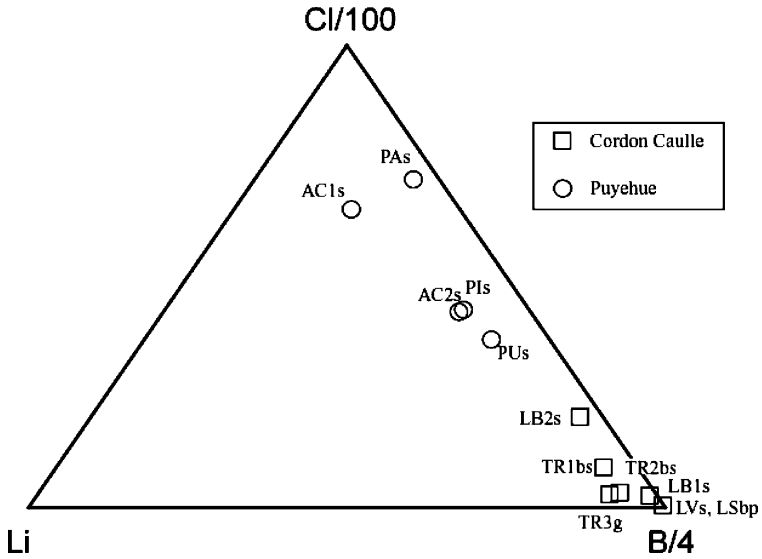

Fig. 4. Cl–Li–B ternary diagram highlighting the distinctive B/Cl ratios of Cordón Caulle and Puyehue.

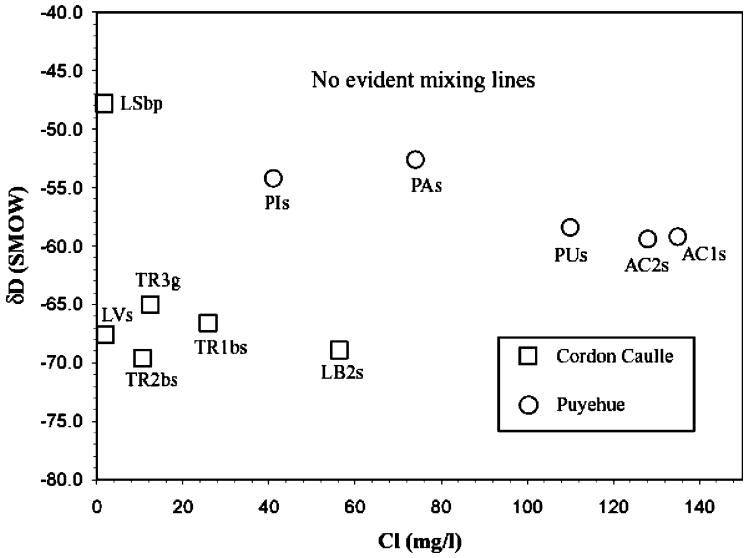

Fig. 5. The Cl–δD plot showing no apparent mixing trends between Puyehue and Cordón Caulle.

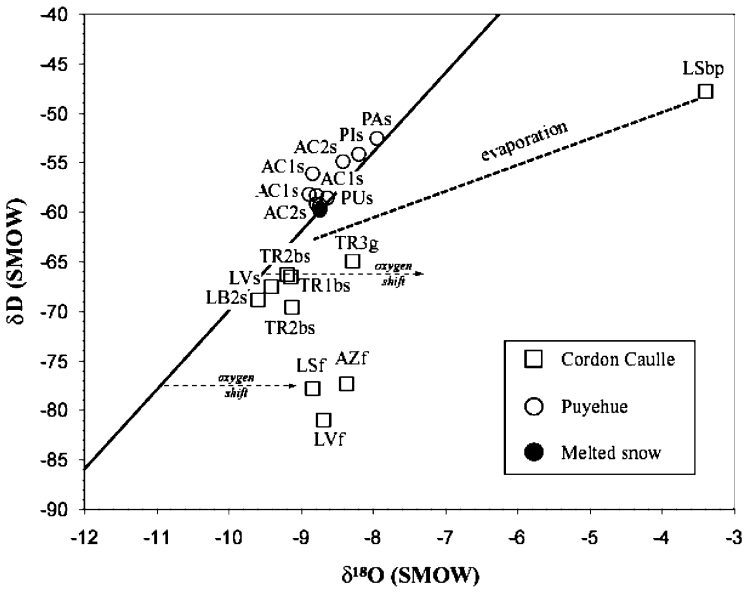

Fig. 6. The $\delta^{18}O$–δD plot showing the isotopic composition of fumarole condensates, thermal springs and melted snow for Puyehue-Cordón Caulle, relative to the GMWL, with V-SMOW standard.

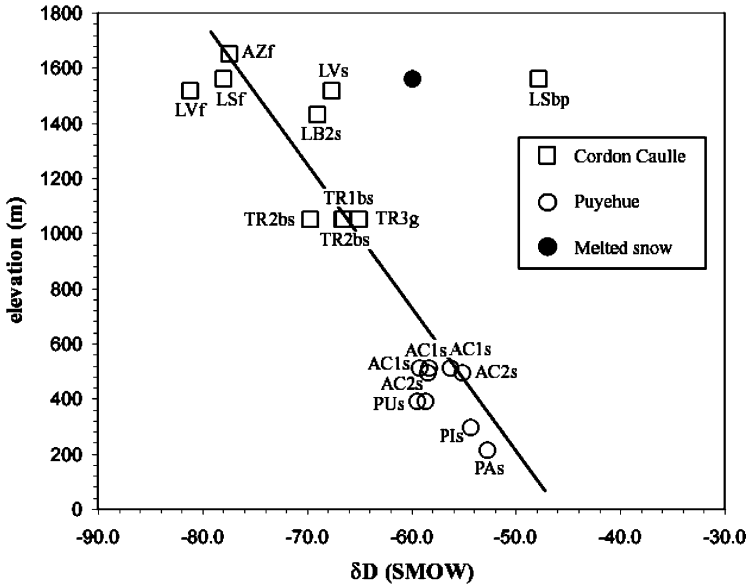

Fig. 7. The δD–elevation plot showing the linear correlation between δD in the thermal discharges and elevation, defining a deuterium gradient of −19.4 (per million)/1000 m. Note that melted snow does not fit this linear trend.

used to address the connection between Cordón Caulle and Puyehue. Note that no evident mixing trends can be delineated.

The isotopic composition of the waters is plotted relative to the global meteoric water line (GMWL; Craig, 1963; Fig. 6). All the springs from Puyehue are aligned close to the GMWL, whereas Cordón Caulle samples show a variable δ^{18}O-shift relative to the GMWL. The greatest δ^{18}O-shift is that of Las Sopas, interpreted as an evaporation trend. Melted snow is used as reference for the local meteoric or recharge composition of Cordón Caulle. With the exception of melted snow, δD values in the thermal discharges show a linear correlation with elevation (Fig. 7), defining a deuterium gradient of −19.4 (per million)/1000 m.

5. Discussion

5.1. Water chemistry

By the early 1970s, drilling at El Tatio, Puchuldiza and Surire, in northern Chile, had provided evidence that all existent chloride-rich (∼1000 ppm) springs were the surface manifestation of deep neutral-chloride waters with temperatures as high as 250 °C (Lahsen and Trujillo, 1975; Lahsen, 1976). Similar findings in a number of geothermal areas worldwide support the current belief that chloride is a potential indicator of deep high-enthalpy, liquid-dominated geothermal systems in a volcanic setting (Giggenbach and Goguel, 1989). Water-rock interaction (Ellis and Mahon, 1964, 1967) and absorption of magmatic HCl into deep-circulating groundwater (e.g. Giggenbach, 1988) are among the mechanisms

supplying chloride to the hydrothermal solutions. Once added either from rock dissolution or magma degassing (or both), chloride preferentially resides in the liquid phase as dictated by its non-volatile and conservative character at geothermal conditions (<300 °C; e.g. Giggenbach, 1997). In a steep volcanic terrain associated with a liquid-dominated system, the discharge of chloride-rich springs is favorable in areas where the regional water table is shallow or superficial (e.g. Henley et al., 1984). At Trahuilco (∼1000 m), where this favorable condition is more than sufficient, the large outflow (nearly 100 l/s) of low chloride springs (<60 mg/l) points to the existence of a secondary steam-heated aquifer overlying a main vapor-dominated reservoir. Chloride, if existent, is likely to have remained at depth, forming part of a relatively immobile brine. Boron, which is more volatile than chloride at geothermal conditions (Giggenbach and Goguel, 1989), may have partitioned into steam during deep boiling, probably as H_3BO_3, together with CO_2 and other gas species. Partial absorption of B and CO_2 into this secondary aquifer seems compatible with the relatively high B/Cl ratios (Fig. 4) and the higher $HCO_3^- + CO_3^{2-}$ relative to SO_4 and Cl (Fig. 3) in the Trahuilco springs, respectively.

At Puyehue, both surface temperatures and Cl/HCO_3 ratios (Fig. 3) decrease northward with decreasing elevation, from Aguas Calientes to Pangal-Pichichanleufu, pointing to a concealed outflow flowing from south to north. This, together with the contrasting B/Cl ratios between Cordón Caulle and Puyehue, the lack of mixing trends in the Cl–δD plot (Fig. 5) and the outflow at Cordón Caulle in a SE–NW direction, suggests that Cordón Caulle and Puyehue represent two separate upflows.

5.2. Isotopic composition

The positive $\delta^{18}O$-shift of the thermal discharges from Cordón Caulle relative to the GMWL (Fig. 6) is probably related to an active geothermal system. Craig (1963) presented evidence from a number of geothermal areas that thermal waters undergo a progressive $\delta^{18}O$-enrichment with respect to the GMWL, as a result of water-rock oxygen exchange, and that δD values remain relatively constant throughout this process. More recently, Giggenbach (1992) showed a positive shift in both $\delta^{18}O$ and δD with respect to the local meteoric composition in several thermal areas, ascribed to mixing of local meteoric and andesitic (magmatic) waters. However, these studies do not document any negative δD-shift relative to the local meteoric composition, such as that of the thermal discharges of Cordón Caulle relative to melted snow (local meteoric composition). In this regard, it is possible that:

(1) the only measurement of melted snow may not correctly represent the fluid recharging Cordón Caulle. The deuterium gradient of −19.4 (per million)/1000 m inferred from the linear correlation between δD values and the elevation (Fig. 7) suggests that much of the relative δD variations in the thermal discharges from Puyehue-Cordón Caulle are inherited from the original recharge waters. For comparison, the variation of deuterium with elevation at equatorial latitudes is described by a deuterium gradient of −16.2 (per million)/1000 m (Aravena, 2003, personal communication). The fact that melted snow departs from the δD-elevation linear trend (Fig. 7) gives some insight into the existence of further recharge sources such as rainfall water or surface runoff, eventually differing in composition from melted snow.

(2) The original δD signature of the recharge waters, likely to be retained in a deep reservoir liquid, can be modified in response to boiling-related isotopic fractionation (Giggenbach and Stewart, 1982). Consequently, the δD-elevation linear correlation may be overestimated by the presence of fumarole condensates (steam). If this is the case and the connection between melted snow and the recharge is correct, the particular and unusual δD depletion in the Trahuilco springs relative to melted snow could be attributed to the mixture of groundwater (melted snow) and deep-formed steam (fumarole condensates) at shallow depth, which is compatible with a steam-heated origin. Note that the composition of deep-formed steam can differ from that of fumarole condensates in close proportion to shallow steam condensing.

5.3. Geothermometry

Solute geothermometers, including those based upon silica solubility and Na/K and K^2/Mg ratios (e.g. Fournier, 1985; Giggenbach, 1988), are ideally applied to chloride springs but considered less reliable when applied to low-chloride springs like those of Puyehue and Cordón Caulle. Bearing this in mind, a range of silica and cation temperatures is listed in Table 1. Temperatures are not reported at Las Sopas, where the composition of the acidic pools is likely to reflect only surface processes largely associated with the dissolution of country rocks, nor at Los Venados and Los Baños (∼1500 m). In the latter, the existence of bicarbonate springs with relatively low flow rates emerging from unconsolidated pumice layers points to the existence of shallow perched aquifers where silica solubility is probably controlled by the dissolution of volcanic glass. The temperatures calculated at Trahuilco are considered the most reliable indicators, due to the vigorous flow rates observed. The ability of the Trahuilco springs to retain SiO_2 (aq) is greatly enhanced by their alkaline pH (>8.5), in accordance with the dissociation of silicic acid:

$$H_4SiO_4{}^{\circ} = H_3SiO_4{}^{-} + H^{+} \tag{1}$$

where $K = [H_3SiO_4{}^{-}][H^{+}]/[H_4SiO_4]$, with [ ] = activity. The temperature dependence of the dissociation constant K is given by:

$$\log K = \frac{-2549}{t} - 15.36 \times 10^{-6} \times t^2 \tag{2}$$

with t in [Kelvin] (e.g. Arnórsson, 2000). Assuming that $\gamma_{H_3SiO_4{}^{-}} \sim 1$, the fraction of $H_3SiO_4{}^{-}$ is calculated as a function of the SiO_2(total), pH and temperature using the formula:

$$H_3SiO_4{}^{-} = \frac{SiO_2(\text{total})}{(10^{-pH}\gamma_{H_3SiO_4{}^{-}}/K) + 1} \tag{3}$$

(Fournier, 1985) where $SiO_2(\text{total}) = H_3SiO_4{}^{-} + H_4SiO_4$ (Table 1), and $\gamma_{H_3SiO_4{}^{-}}$ is the activity coefficient of $H_3SiO_4{}^{-}$, which is calculated using the extended form of the Debye-Hückel equation (Helgeson et al., 1981; Henley et al., 1984):

$$-\log \gamma_i = \frac{Az^2 I^{1/2}}{1 + \mathring{a}bI^{1/2}} + BI \tag{4}$$

with the selected parameters $z = -1$ (ionic charge of $H_3SiO_4^-$); å $= 4.0 \times 10^{-8}$ cm (ion size parameter of $H_3SiO_4^-$); *A* and *B* are Debye-Hückel coefficients for water at vapor pressure, interpolated from Helgeson et al. (1981) as a function of temperature; and $I = 0.005$ (ionic strength at TR2bs; Appendix B). Between 100 and 25 °C, Eq. (4) yields $\gamma_{H_3SiO_4^-} \sim 0.91$, showing little impact on the pH correction (Eq. (3)), as expected in dilute waters.

At Trahuilco, the pH has been measured at discharge and room temperature (in samples TR1bs, TR2bs and TR3g), showing negligible variations. In the spring vent areas, however, pH may change over time, specially if sulfide (easy to detect by its "rotten egg" smell) oxidation occurs or if CO_2 begins to be absorbed back from the atmosphere. Ignoring these possible pH changes, the fraction of H_4SiO_4 is modeled as a function of temperature (92–25 °C, Eq. (3)), for constant SiO_2(total) (Fig. 8). The fraction of H_4SiO_4 is projected to rise with cooling, intercepting the amorphous silica saturation curve (Fournier, 1985) at about ~60–70 °C (Fig. 8). This is thought to describe a possible path for silica sinter deposition. Although saturation with respect to Opal-CT would be attained earlier, as predicted from the Opal-CT solubility curve (Fournier, 1985; Appendix B), the XRD data do not support the presence of Opal-CT at the surface (Appendix A). Two pH-corrected silica temperatures are presented in Table 1 (samples TR2bs and TR3g), corresponding to H_4SiO_4 calculated at 25 and 92 °C. The ambiguities in the pH correction are greater at TR3g because of the wide variations of H_4SiO_4 between 92 and 25 °C (Fig. 8).

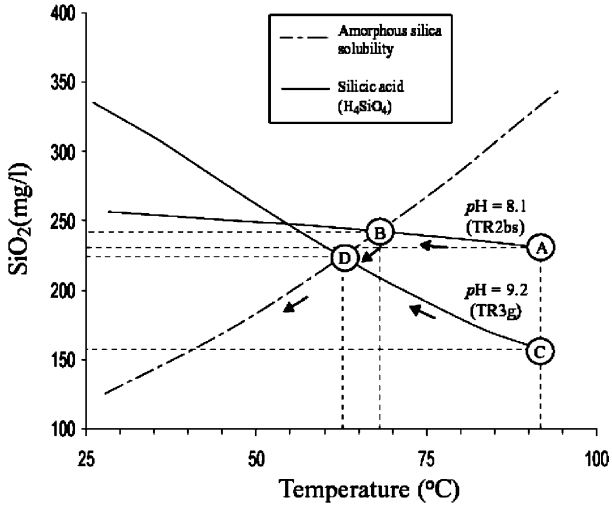

Fig. 8. Variation of H_4SiO_4 with temperature as dictated by the silica dissociation constant (see text) and the pH correction, taking a constant $SiO_{2\,total}$ of 259 mg/l at TR2bs and of 409 mg/l at TR3g. Discharge conditions (92 °C) are described by points A ($H_4SiO_4 \sim 229$ mg/l, 89% of $SiO_{2\,total}$) and C ($H_4SiO_4 \sim 156$ mg/l, 38% of $SiO_{2\,total}$), both undersaturated with respect to amorphous silica. Under natural conditions, attainment of amorphous silica saturation is predicted to take place at about 60–70 °C (point B: $H_4SiO_4 \sim 240$ mg/l, 94% of $SiO_{2\,total}$; point D: $H_4SiO_4 \sim 224$ mg/l, 55% of $SiO_{2\,total}$), after which the thermal waters are likely to follow the amorphous silica saturation curve with further cooling (Fournier, 1985).

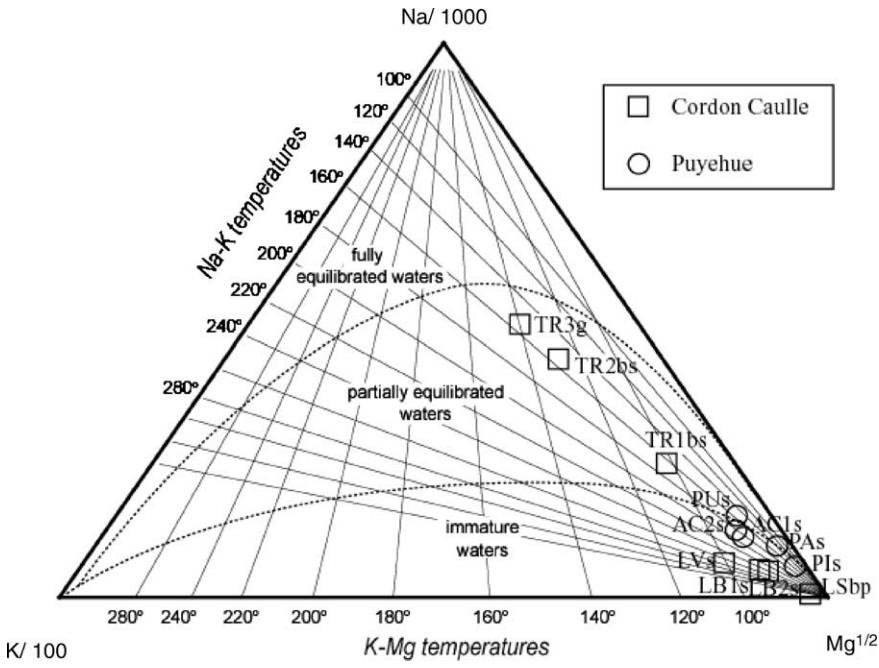

Fig. 9. Na–K–Mg ternary diagram showing the impact of dilution on the Puyehue springs. Na–K temperatures at Trahuilco, where a partial equilibrium condition is inferred, are estimated to approach the subsurface temperatures of the secondary aquifer.

In the Na–K–Mg ternary diagram (Fig. 9), fully equilibrated samples are defined as those yielding similar Na–K and K–Mg temperatures (Giggenbach, 1988). Samples depart from the full-equilibrium condition towards the Mg corner as a result of either fast re-equilibration of the K–Mg geothermometer with decreasing temperature or dilution (meteoric waters and normally Mg-rich), or both. On the basis of the high relative Mg concentration in the Puyehue springs (Fig. 9) and their isotopic composition resembling the local meteoric composition (Fig. 6), a strong impact of dilution is thought to dominate at Puyehue. At Cordón Caulle, dilution is not the only explanation for the elevated Mg. In the acidic waters of Las Sopas, Mg can be linked to rock dissolution. At Trahuilco, absolute Mg concentrations are much lower (<0.06 mg/l) than those of cold rivers and springs (e.g. Nilahue river, 3.1–10.2 mg/l; Riñinahue river, 1.2–5.2 mg/l; Fig. 2). In agreement with the partial equilibrium condition suggested by the Na–K–Mg diagram for Trahuilco (Fig. 9), the apparent removal of Mg from solution (if steam-heated in origin) can be attributed to fluid-mineral equilibrium between Mg-chlorite, adularia, illite and chalcedony at shallow depth. The faster re-equilibration of the K–Mg system relative to the Na–K system (Giggenbach, 1988) suggests that K–Mg temperatures at Trahuilco, in the range 100–140 °C, are closer to discharge conditions, whereas the Na–K temperatures in the range 155–165 °C (Table 1; Fig. 8) best approach the equilibration temperatures of the secondary steam-heated aquifer.

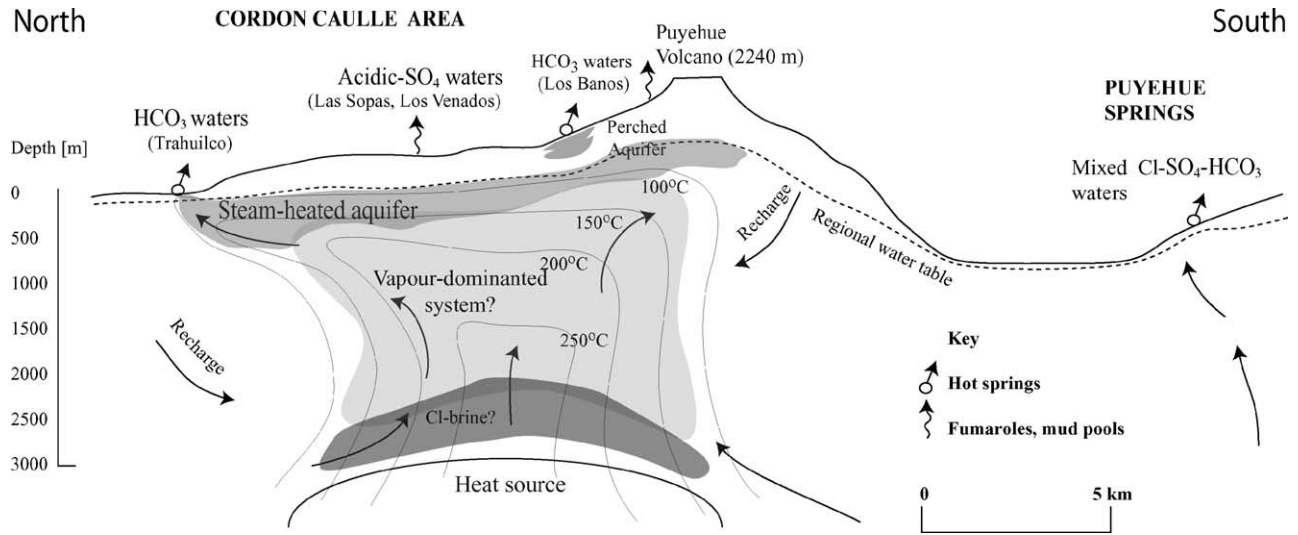

Fig. 10. Conceptual model of the Puyehue-Cordón Caulle system, showing a vapor-dominated system in Cordón Caulle, with a secondary steam-heated aquifer and an immobile Cl-brine at depth. Isotherms have been approximated from solute geothermometers for the steam-heated aquifer at Cordón Caulle and extrapolated to greater depths.

If steam-heated in origin, the Trahuilco springs circulate at shallow depth through pyroclastic rocks and lavas, where silica solubility could be controlled either by volcanic glass or chalcedony (due to rapid glass devitrification), but less probably by quartz. In general, there is a strong disagreement between quartz and Na–K temperatures in Trahuilco (with the only exception of TR3g, pH-correction at 92 °C; Table 1), giving a hint that quartz temperatures (up to 241 °C; Table 1) may be overestimated. Chalcedony temperatures in the range 170–180 °C, as calculated for TR2bs (where ambiguities associated with the pH correction are minor), are suggested to best represent the subsurface temperatures at the secondary steam-heated aquifer. At Puyehue, Na–K temperatures in the range 150–180 °C are systematically higher than silica temperatures, probably reflecting the greater immunity of ratio-based geothermometers to dilution relative to single constituent-based geothermometers. However, it is worth recalling that the Na–K system is best applied to chloride-rich waters equilibrated at >180 °C, suggesting a conservative interpretation of cation temperatures at Puyehue.

6. Concluding remarks

The surface manifestations of the Puyehue-Cordón Caulle thermal area correspond to two distinctive geothermal systems. These two systems are unusual in the overall absence of chloride-rich springs. At Cordón Caulle, in the Trahuilco area, the large outflow of bicarbonate springs points to a vapor-dominated system, overlain by a secondary steam-heated aquifer with equilibration temperatures of about 170–180 °C, as estimated from corrected silica geothermometers. The isotopic data also indicate a steam-heated origin at Trahuilco, although the composition of the recharge waters still remains uncertain. A conceptual model of the Puyehue-Cordón Caulle system has been developed on the basis of the reported chemical and isotopic data (Fig. 10). Gas geothermometry and geophysical surveys, including electric or magnetotelluric methods, are strongly recommended in order to refine this model.

Acknowledgements

This study forms part of the FONDEF Grant No. 1051 of CONICYT (National Council of Science and Technology Research, Chile): “Characterization and Assessment of Geothermal Resources of Central and Southern Chile: Possibilities of Generation of Electric Energy and Direct Applications”. The authors would also like to thank CONICYT for support through Ph.D. fellowships and stages abroad. Thanks are extended to: the International Bureau of the Federal Ministry of Education and Research, Germany; Tom Powell (Thermochem, USA); Luis Urzúa, David Sussman, Juan Rojas (ENAP, Chile); Pablo Letelier, Jaime Martínez (Department of Geology, University of Chile); Walter Glaesser (UFZ, Germany); Stefan Wohnlich (University of Munich, Germany); Stuart F. Simmons, Patrick Browne, Mark Simpson (Geothermal Institute, The University of Auckland, New Zealand); Javier Labra, Nicolás Pacheco (CONAF National Park Puyehue, Chile); Bill Evans (USGS), and an anonymous reviewer.

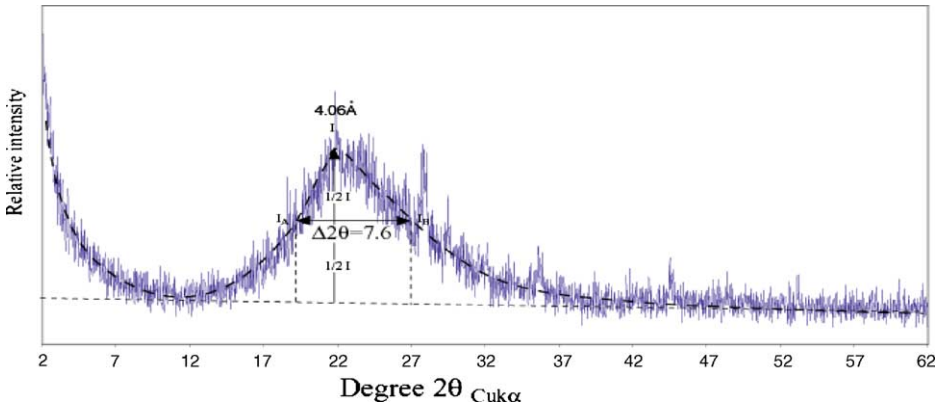

Fig. A.1. XRD pattern for silica sinter at Trahuilco, showing that Opal-A is the dominant variety of silica in the sinters.

Appendix A. XRD pattern of silica sinters from Trahuilco

Silica powder scanning was carried out at 1°/min with a step size of 0.02° from 2 to 62° 2θ, under a selected voltage and current of 40 kV and 20 mA, respectively. The resulting XRD pattern (Fig. A.1) shows a band of moderate intensity centered at 4.06 Å, with a band width of 7.6° 2θ. The band width is calculated as the difference between the positions of the half maximum intensities, $I_A - I_B$ (=27 − 19.4° 2θ). Opal-A is typified by a broad band centered about 3.90–4.13 Å and band widths ranging from 6.3 to 8.3° 2θ, with a mean of 7.3° 2θ (Herdianita et al., 2000a,b). For comparison, Opal-CT shows a band of greater intensity centered about 4.04–4.14 Å with an abrupt decrease in the width (0.5–1.7° 2θ) relative to Opal-A. The analyzed diffractogram therefore corresponds to Opal-A.

Appendix B. Geothermometry

B.1. Silica geothermometers (Fournier and Potter, 1982; Fournier, 1985)

$$T = C_1 + C_2\mathrm{S} + C_3\mathrm{S}^2 + C_4\mathrm{S}^3 + C_5 \log \mathrm{S}, \quad \text{Quartz geothermometer (20–330 °C)}$$

$$C_1 = -4.2198 \times 10$$

$$C_2 = 2.8831 \times 10^{-1}$$

$$C_3 = -3.6686 \times 10^{-4}$$

$$C_4 = 3.1665 \times 10^{-7}$$

$$C_5 = 7.7034 \times 10$$

$$T = \frac{1032}{(4.69 - \log \mathrm{S})} - 273.15, \quad \text{Chalcedony}$$

Table B.1
Ionic strength calculation for the TR2bs spring

	Atomic weight (g/mol)	Charge, z_i	Concentration (mg/l)	mEq., m_i
Na	23.0	1	101	0.004
K	39.1	1	3.1	0.000
Ca	40.1	2	0.1	0.000
Mg	24.3	2	0.01	0.000
Cl	35.5	−1	11	0.000
B	10.8	0	12.0	0.001
SO_4	96.1	−2	27	0.000
HCO_3	61.0	−1	214	0.004
SiO_2	60.1	0	259	0.004
Ionic strength ($l/2\Sigma m_i z_i^2$)				0.005

TDS = 626 mg/1.

$$T = \frac{781}{(4.51 - \log \mathrm{S})} - 273.15, \quad \text{Opal-CT}$$

$$T = \frac{731}{(4.52 - \log \mathrm{S})} - 273.15, \quad \text{Amorphous silica}$$

where S is the SiO_2 concentration (mg/kg[1]) and T is the temperature in °C (Table B.1).

B.2. Cation geothermometers (Giggenbach, 1988)

$$T\,(^\circ\mathrm{C}) = \frac{1390}{[(1.75 + \log(\mathrm{Na/K}))]} - 273.15, \quad \text{Na–K geothermometer}$$

$$T\,(^\circ\mathrm{C}) = \frac{4410}{[(14 - \log(\mathrm{K}^2/\mathrm{Mg}))]} - 273.15, \quad \text{K–Mg geothermometer}$$

References

Arnórsson, S., 2000. Isotopic and Chemical Techniques in Geothermal Exploration, Development and Use. International Atomic Energy Agency, Vienna.

Campos, A., Moreno, H., Muñoz, J., Antinao, J., Clayton, J., Martín, M., 1998. Mapa geológico del área de Futrono (1:1,000,000). Servicio Nacional de Geología Minería, Chile.

Cembrano, J., Hervé, F., Lavenu, A., 1996. The Liquiñe-Ofqui fault: a long-lived intra-arc fault system in southern Chile. Tectonophysics 259, 55–66.

Cembrano, J., Schermer, E., Lavenu, A., Sanhueza, A., 2000. Contrasting nature of deformation along an intra-arc shear zone, the Liquiñe-Ofqui fault zone, Southern Chilean Andes. Tectonophysics 319, 129–149.

Craig, H., 1963. The isotopic geochemistry of water and carbon in geothermal areas. In: Nuclear Geology of Geothermal Areas, CNR, Pisa, Italy, pp. 17–53.

[1] mg/l can be used instead without introducing significant error, because of the low salinity of the solutions in question.

Ellis, A.J., Mahon, W.A.J., 1964. Natural hydrothermal systems and experimental hot water/rock interactions. Geochim. Cosmochim. Acta 28, 1323–1357.

Ellis, A.J., Mahon, W.A.J., 1967. Natural hydrothermal systems and experimental hot water/rock interactions (Part II). Geochim. Cosmochim. Acta 31, 519–538.

Fournier, R.O., 1985. The behavior of silica in hydrothermal solutions. Rev. Econ. Geol. 2, 45–62.

Fournier, R.O., Potter, R.W., 1982. An equation correlating the solubility of quartz in water from 25 to 900 °C at pressures up to 10,000 bar. Geochim. Cosmochim. Acta 46, 1969–1974.

Giggenbach, W., 1988. Geothermal solute equilibria. Derivation of Na–K–Mg–Ca geoindicators. Geochim. Cosmochim. Acta 52, 2749–2765.

Giggenbach, W., 1992. Isotopic shifts in waters from geothermal and volcanic systems along convergent plate boundaries and their origin. Earth Planet. Sci. Lett. 113, 495–510.

Giggenbach, W., 1997. The origin and evolution of fluids in magmatic-hydrothermal systems. In: Barnes, H.L. (Ed.), Geochemistry of Hydrothermal Ore Deposits, 3rd ed. Wiley, New York, pp. 737–796.

Giggenbach, W., Goguel, R., 1989. Collection and Analysis of Geothermal and Volcanic Water and Gas Discharges. Unpublished report, Chemistry Division, Department of Scientific and Industrial Research, Petone, New Zealand, 81 pp.

Giggenbach, W., Stewart, K., 1982. Processes controlling the isotopic composition of steam and water discharges from steam vents and steam-heated pools in geothermal area. Geothermics 11, 71–80.

Hauser, A., 1997. Catastro y Caracterización de Fuentes Termales y Minerales de Chile. Boletín No. 50, Subdirección Nacional de Geología, Sernageomin, Chile.

Helgeson, H.C., Kirkham, D.H., Flowers, G.C., 1981. Theoretical prediction of the behavior of aqueous electrolytes at high pressures and temperatures: calculation of activity coefficients, osmotic coefficients, and apparent molal, and standard and relative partial molal properties to 600 °C and 5 kb. Am. J. Sci. 281, 1249–1516.

Henley R.W., Truesdell, A.H., Barton, P.B., 1984. Fluid-mineral equilibria in hydrothermal systems. Reviews in Economic Geology 1, Society of Economic Geologists, El Paso, TX.

Herdianita, N.R., Browne, P.R.L., Rogers, K.A., Campbell, K.A., 2000a. Mineralogical and textural changes accompanying ageing of silica sinter. Mineralium Deposita 35, 48–62.

Herdianita, N.R., Browne, P.R.L., Rogers, K.A., 2000b. Routine instrumental procedures to characterize the mineralogy of modern and ancient silica sinters. Geothermics 29, 65–81.

Lahsen, A., 1976. Geothermal Exploration in Northern Chile—Summary. Circum-Pacific Energy and Mineral Resources, Memoir No. 25, The American Association of Petroleum Geologists.

Lahsen, A., 1988. Chilean geothermal resources and their possible utilization. Geothermics 17, 401–410.

Lahsen, A., Trujillo, P., 1975. El Tatio geothermal field. In: Chile Proceedings of the 2nd U.N. Symposium Developemental Use of Geothermal Resources, San Francisco, vol. 1, pp. 157–178.

Lara, L., Moreno, H., Lavenu, A., 1999. Volcanism and tectonics of the Pleistocene-Holocene Volcanic Arc, Southern Andes (40.5–41.5°S). In: Proceedings of the Fourth International Symposium on Andean Geodynamics, Göttingen, pp. 417–421.

Lara, L., Moreno, H., Naranjo, J., 2000. Análisis estructural de la erupción fisural de 1960 en el Cordón Caulle (40.5°S) y su relación con el sismo de Valdivia (1960; Mw = 9.5). IX Congreso Geológico Chileno 2, 40–43.

Lara, L., Rodriguez, C., Moreno, H., Pérez de Arce, C., 2001. Geocronología K-Ar y geoquímica del volcanismo Plioceno superior-Pleistoceno de los Andes del Sur (39–42°S). Rev. Geol. Chile 28 (1), 67–90.

López-Escobar, L., Cembrano, J., Moreno, H., 1995. Geochemistry and tectonics of the Chilean Southern Andes basaltic Quaternary volcanism (37–46°S). Rev. Geol. Chile 22, 219–234.

Moreno, H., 1977. Geología del área volcánica de Puyehue-Carrán en los Andes del sur de Chile. Memoria de Título, Universidad de Chile, Departamento de Geología, Santiago, 170 pp.

Pérez, Y., 1999. Fuentes de Aguas Termales y Minerales de la Cordillera Andina del Sur de Chile (39–42°S). Boletín No. 54, Subdirección Nacional de Geología, Sernageomin, Chile.

Rodgers, K.A., Cook, K.L., Browne, P.R.L., Campbell, K.A., 2002. The mineralogy, texture and significance of silica derived from alteration by steam condensate in three New Zealand geothermal fields. Clay Miner. 37, 299–322.